Review
Particulate silicon nitride-based composites

Yu. G. GOGOTSI*
*Tokyo Institute of Technology, Research Laboratory of Engineering Materials,
4259 Nagatsuta, Midori-ku, Yokohama 227, Japan*

In an attempt to optimize the structure and properties of silicon nitride ceramics, a variety of novel processing techniques and materials compositions have evolved over the last 15 years. Among the most important, was the development of various silicon nitride-based composites. A review of particulate, silicon nitride-based composites other than whisker- or platelets-reinforced, is presented. Materials based on silicon nitride and SiAlONs, with additions of carbides, nitrides and borides of transition metals are described. Special emphasis is placed on TiN- and TiC-containing ceramics. The manufacture of composites by hot pressing, reaction sintering, pressureless and gas-pressure sintering is discussed. The data on properties, including conductivity, density, Young's modulus, strength, fracture toughness, hardness, thermal expansion, wear, creep and oxidation resistance are presented. Analysis of actual and potential uses of the selected composites demonstrates that the particulate composites are very promising as tool, structural and electronic materials.

1. Introduction

In the last 20 years, ceramics have won increasing importance for engineering applications despite their inherent brittleness [1–3]. Because of their high strength, hardness and thermal stability, silicon nitride ceramics are among the most important materials for structural applications. The need for further improvement in the mechanical reliability of silicon nitride has recently led to the development of high-strength and high-toughness ceramics, such as fibre-, whisker- or particulate-reinforced ceramics [4–6]. Owing to process problems and the cost of whiskers and fibres, however, increased attention is being devoted to particulate composites [7]. Silicon carbide was used as an addition to Si_3N_4 more than 20 years ago [8]. However, the use of SiC as uniform particles cannot improve noticeably the properties of the matrix [5, 9]. Therefore, SiC is used mostly in the form of whiskers, fibres and platelets. These materials were extensively studied and will not be discussed in the present work.

A major focus of this review is on the composites containing nitrides, carbides or borides of transition metals in the silicon nitride, silicon oxynitride or SiAlON matrix. The thermal expansion mismatch between added particles and the Si_3N_4 matrix can produce compression stresses in the matrix during cooling after sintering, thus improving the mechanical properties. Si_3N_4 is hard to work and cannot be subjected to electro-discharge machining (EDM) because of its insulating properties. On the other hand, nitrides and carbides of transition metals generally have as

high an electrical conductivity as that of metals. The addition of a conductive phase, such as Ti(N,C) or Zr(N,C), makes possible EDM of the ceramics and their use for some specific electrotechnical applications. New conductive silicon nitride- and SiAlON-based composites were developed for these purposes by adding amounts of TiC, TiN or TiCN particles to the ceramic matrix. These composites have been considered for heaters, cutting tools, wear-resistant and structural components.

Knowledge of the effects of the kind, grain size and content of particulate additions on the properties of silicon nitride is essentially important for development of new materials, combining high mechanical properties and necessary electrophysical characteristics. However, no attempts to describe the availability in the scientific literature data on such materials have been made previously.

The main objective of this review was to evaluate the effects of the content and grain size of particulate additions on processing, structure and properties of silicon nitride- and SiAlON-based ceramics produced by various technological routines (sintering, hot pressing and reaction sintering). It summarizes both the literature and the author's own results of investigations in a sufficiently comprehensive form. This contribution looks into the promising concepts for improving mechanical, chemical and electrophysical properties of ceramics. A number of aspects are touched upon, for example, the technological performance of such composites, promising compositions,

* *Permanent address*: Institute for Problems of Materials Science, Kiev, Ukraine.
Present address: University of Oslo, Centre for Materials Research, 0371 Oslo, Norway.

property values achieved to date, practical application and relative potentials for particulate composites.

2. Basic principles

The selection of compounds to modify the silicon nitride matrix provides some degrees of freedom. However, several primary criteria must be fulfilled. These are:

(i) chemical compatibility with the matrix;

(ii) moderate difference in thermal expansion coefficients;

(iii) high electrical conductivity (in case of EDM-machinable and electroceramics);

(iv) environmental stability (in case of structural materials);

(v) low cost.

2.1. Chemical compatibility with silicon nitride

Various nitrides, carbides and borides of transition metals can be added to silicon nitride [10]. Work on TiC-containing composites was initiated in the 1970s [11–14] and continued in the 1980–90s [6, 15–19]. It has been shown [16] that the reaction between the Si_3N_4 matrix and TiC results in the formation of SiC and titanium carbonitride
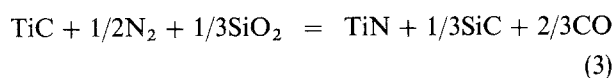
$$Si_3N_4 + 6TiC = 3SiC + 6TiC_{0.5}N_{0.5} + 1/2N_2 \tag{1}$$
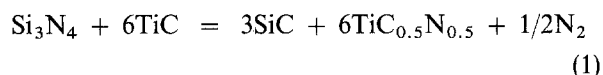
At the sintering temperature, the reaction can proceed $(\Delta G = -30 \, Kcal \, mol^{-1})$ until all TiC is consumed. Reaction 1 is sensitive to the partial pressure of nitrogen [19]. The reaction is possible only when the partial pressure of nitrogen during sintering is lower than that for the equilibrium
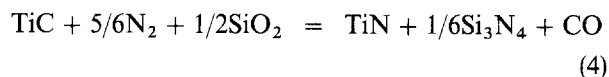
$$3SiC + 2N_2 = Si_3N_4 + 3C \tag{2}$$
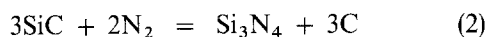
At low pressures, TiN can be formed. However, in most cases titanium carbonitride, TiC_xN_{1-x}, with x values from 0 to 0.5, was found.

TiC reacts also with silica, which is always present on the surface of the Si_3N_4 particles, according to the reaction

$$TiC + 1/2N_2 + 1/3SiO_2 = TiN + 1/3SiC + 2/3CO \tag{3}$$

or

$$TiC + 5/6N_2 + 1/2SiO_2 = TiN + 1/6Si_3N_4 + CO \tag{4}$$

at high nitrogen pressures, when SiC is unstable. It follows from Equations 3 and 4, that the rate of the decomposition of TiC also depends on the CO content in the sintering atmosphere and on the silica content in the powder mixture.

Thus, the interaction between the matrix and TiC leads to substantial changes in the phase composition of the materials. This was a reason why in the 1980s the use of TiN [20–35] and $TiC_{0.5}N_{0.5}$ [36–38] for substitution of TiC was proposed. Thermodynamic calculations [19] demonstrated that TiN is stable in the temperature range that is used for sintering of Si_3N_4. Only small changes in nitrogen content, depending on the nitrogen partial pressure, are possible. However, according to the published data, up to 7 wt % Si_3N_4 can be dissolved in TiN at 1650 °C [39] and up to 30 at % Ti can be dissolved in Si_3N_4 at 1725 °C [40]. The formation of the solid solution of Si_3N_4 in TiN under equilibrium conditions in the real systems seems to be hindered by the presence of intergranular silicate phases.

In addition to TiC, TiN and TiC_xN_{1-x}, some other compounds, for example ZrN [36, 37], ZrC [41], TiB_2 [42], BN [43], NbC, TaC, $TaSi_2$, TaN, HfC [14], were used for modifying the structure of Si_3N_4. The properties of some of them are summarized in Table I. Not all nitrides and carbides of transition metals can coexist with Si_3N_4. For example, ZrC_xN_{1-x} $(0 < x < 0.32)$ can coexist with Si_3N_4 at 1650 °C [44], but CrN and Cr_2N react with Si_3N_4 with the formation of Cr_5Si_3 even in a nitrogen atmosphere [45, 46]. Generally, nitrides have better compatibility with Si_3N_4 than carbides: the latter can react with Si_3N_4 with the formation of SiC.

2.2. Improvement of mechanical properties

A high level of mechanical properties is essential for engineering ceramics. The alteration of Si_3N_4 through dispersed additions with high Young's modulus offers a potential for improvement of the composite's mechanical properties. The theoretical basis for dispersion toughening of ceramics was developed in the 1970–80s and a number of models were proposed [47–56]. The

TABLE I Properties of silicon nitride and some of the refractory compounds used as dispersoids (after [57, 58, etc.])

Compound	Density $(g \, cm^{-3})$	Resistivity (Ωm)	Microhardness (GPa)	Thermal expansion coefficient (K^{-1})	Young's modulus (GPa)
Si_3N_4	3.21	$10^{11}–10^{12}$	30	3.25×10^{-6}	280–320
TiN	5.44	3.34×10^{-7}	20.5	8.0×10^{-6}	430–469
ZrN	7.09	1.8×10^{-7}	16.7	7.24×10^{-6}	
TiB_2	4.48	9×10^{-8}	33.7	4.6×10^{-6}	571
ZrB_2	6.17	1.3×10^{-7}	22.5	5.9×10^{-6}	350
ZrC	6.73	4.9×10^{-7}	29.5	7.0×10^{-6}	355
TiC	4.93	6.1×10^{-7}	31.7	7.95×10^{-6}	427

basic toughening concepts that can be realized in the silicon nitride–refractory compound systems are listed below.

2.2.1. Toughening and strengthening mechanisms

1. Prestressing of the matrix due to differences in thermal expansion of the particles, α_p, and the matrix, α_m. For the case of a single, spherical particle of radius R in an infinite isotropic matrix, a uniform stress, σ^r, arises within the particle and radial and tangential stresses of $\sigma^r R^3/r^3$ and $\sigma^r R^3/2r^3$, respectively, arise in the matrix, where r is the distance from the centre of the particle to a point of the matrix. The stress σ^r can be calculated according to

$$\sigma^r = (\alpha_m - \alpha_p)\Delta T \left/ \left(\frac{1 + v_m}{2E_m} + \frac{1 - 2v_p}{E_p} \right) \right.$$

(5)

where ΔT is the temperature range over which no relaxation of stresses at cooling occurs ($\sim 1200\,^\circ$C for silicon nitride matrices), E is the Young's modulus, v is Poisson's ratio. When $\alpha_p > \alpha_m$, cooling from the sin-

tering temperature puts the particle in tension and the matrix in compression, as is schematically shown in Fig. 1. This residual stress state tends to divert an advancing crack around the dispersoid [50], as shown in Fig. 1b. The α values of the carbides and nitrides of transition metals are higher than that of Si_3N_4 (Table I). Thus, this mechanism can work in the composites under study.

2. Crack deflection or multiplication around or through a particle due to the orientation of preferred fracture surfaces (weak grain boundaries, cleavage planes, etc.).

3. Crack impediment by the ductile particles. This mechanism can lead to an increase of the fracture toughness at elevated temperatures, because of a lower brittle–ductile transition temperature for most nitrides and carbides in comparison with Si_3N_4 (e.g. 800–900 °C for TiC [59]).

4. Crack bowing, which originates from resistant dispersoid particles in the path of a propagating crack. The crack tends to bow between the particles [48].

5. Microcracking due to property (thermal expansion and elastic modulus) mismatches. Theoretical prediction [56] shows that for the Si_3N_4–TiN system, microcracking is possible at high TiN contents (> 60 vol %) and large grain size of TiN ($\sim 100\,\mu$m). Another evaluation [35, 60] gives the critical dimension for spontaneous microcracking equal to 17 μm. In real systems, the microcracking is strongly affected by the energy of the grain boundaries TiN/Si_3N_4, Si_3N_4/glass and Si_3N_4/Si_3N_4. Sintering additives and different processing conditions can alter this energy, thus affecting the critical grain size. This might be the main reason for the observed variations in predicted and experimentally measured values. It remains to be demonstrated, whether or not one can control the size and spacing of microcracks to increase the strength and/or fracture toughness of the composite above the level of the matrix alone.
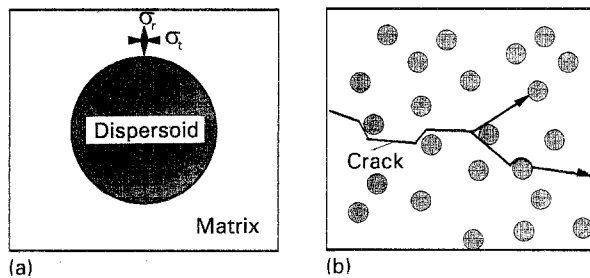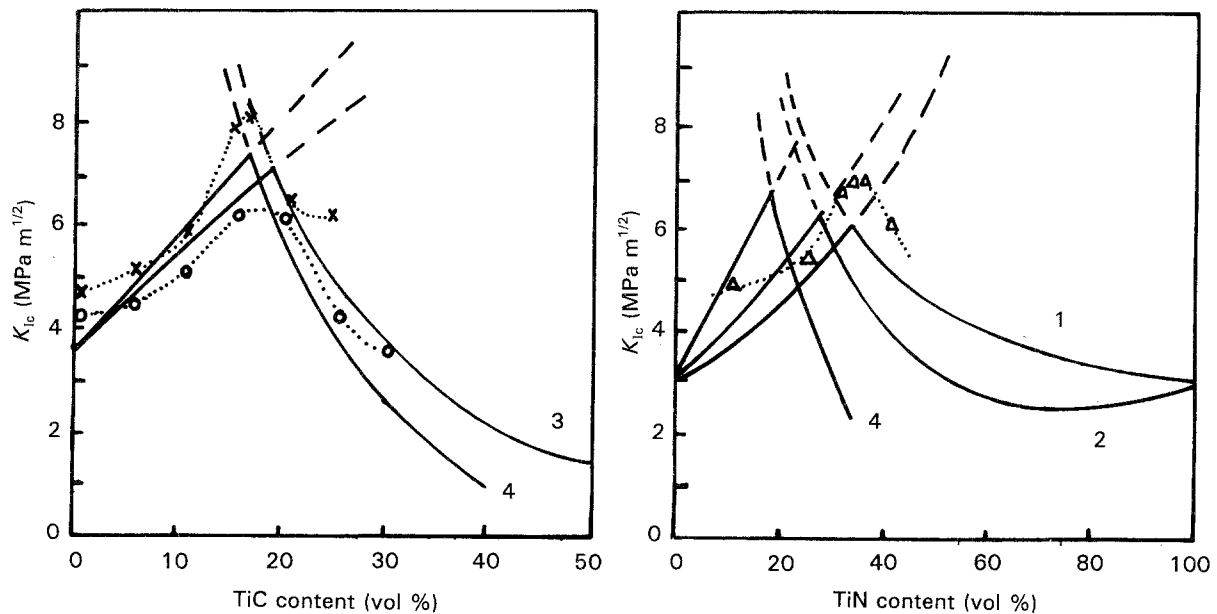

Figure 1 (a) Schematic presentation of the stressed state around the particle, and (b) resulting crack surface roughening and crack tilting and twisting during propagation around dispersoid caused by thermal expansion and elastic modulus mismatch stresses.

Figure 2 (——) Calculated after [56] and ($\bigcirc$, $\triangle$) experimental K_{1c} values for the systems (a) β-SiAlON–TiC and (b) β-SiAlON–TiN: ($\bigcirc$) notched bar; ($\triangle$, $\times$) indentation. σ^{rs}: 1, 0; 2, $\neq 0$, $c = 10\,\mu$m; 3, $\neq 0$, $c = 100\,\mu$m; 4, $\neq 0$, $c = 50\,\mu$m.

While there is often uncertainty in evaluating the main mechanism in a given composite, it is important that typically more than one mechanism is involved. Crack bowing and the crack deflection processes take place simultaneously. The multiplicity of mechanisms provides additional opportunity for design and improvement of composites. However, a theoretical prediction [50] demonstrated that in the case of spherical particles, only a 40%–70% increase of toughness can be achieved. Thus, particulate composites cannot offer as spectacular toughening effect as do whiskers or fibres.

Galanov and Grigor'ev [56] proposed a criterion for the evaluation of the fracture toughness of the composites with internal stresses

$$K_{Ic} = \min_{s} (\alpha_s^{-1} K_{Ic}^s - Y\sigma^{rs}c^{1/2}) \qquad (6)$$

where α_s is the relation of the shear moduli of the component s and the composite $(\alpha_s = G_s/G)$, Y is a geometrical factor, σ^{rs} is the residual stress in the component s, and c is the half length of the crack.

Using the modified Equation 6

$$K_{Ic}^0 = \max_{V_s}, \min_{s} (\alpha_s^{-1} K_{Ic}^s - (2/\pi^{1/2})\sigma^{rs}c^{1/2}) \quad (7)$$

the optimum values (V_s) of the TiN and TiC contents in the β-SiAlON matrix, corresponding to the maximum fracture toughness, were calculated. The maximum level of the fracture toughness is expected to be achieved at ~ 30 vol % TiN or 20 vol % TiC (Fig. 2), which is in agreement with the experimental data.

3. Processing

From a technological standpoint, the processing of particulate composites is much easier and cheaper than the production of fibre- or whisker-reinforced ceramics. All methods, which are used for producing monolithic silicon nitride ceramics, can be applied to the particulate composites. The only problem which was stressed in some investigations [26, 35] is the agglomeration of the added particles, leading to the formation of 50–300 μm aggregates, which can decrease the strength of the composites. A settling of the powder suspensions in an ultrasonic bath or additions of surface-active organic compounds can be proposed for controlling the grain size of TiN. The use of composite Si₃N₄–TiN powders produced by plasmo-chemical synthesis [61] can also improve the homogeneity of the materials.

3.1. Hot pressing

Hot pressing was used for manufacturing Si₃N₄–TiN [26], Si₃N₄–TiB₂ [42] and Si₃N₄–TiC [23] composites. The hot pressing can be carried out in CO [13, 26] or under vacuum [35].

We shall regularly use in the following part of the paper the results obtained on hot-pressed Si₃N₄ (HPSN) with 5 wt % Y₂O₃ + 2 wt % Al₂O₃ as sintering aids and 0–50 wt % TiN (Fig. 3) for illustrating the effects of the content and grain size of particulate additions on the properties of the composite. These
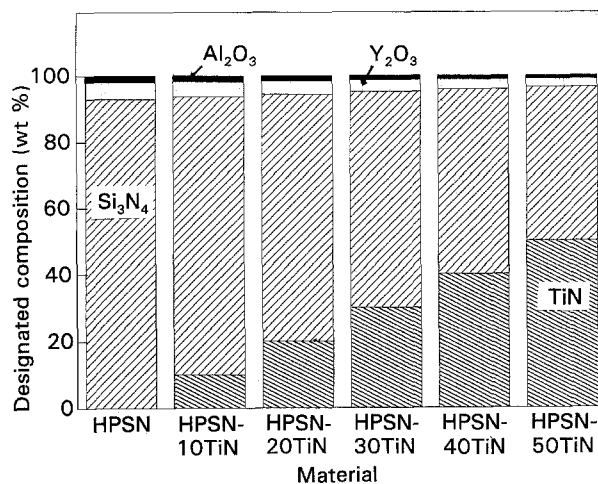

Figure 3 Composition of the Si₃N₄–TiN composites, developed at the Institute for Problems of Materials Science (Kiev, Ukraine).

mixtures were prepared by milling Si₃N₄ with oxide additives in a ball mill to obtain a uniform distribution of oxide additives. A commercial TiN powder was classified by sedimentation into average particle sizes $d_{50} = 0.83, 2.43, 16.8$ and 36.8 μm and carefully mixed with the oxide-doped silicon nitride. Some mixtures were prepared by prolonged milling of TiN in a ball mill together with silicon nitride to obtain a homogeneous distribution of TiN particles in sintered bodies [26, 33]. These materials (HPSN–TiN throughout the text) can serve well as model compositions for the investigation of the effects of the grain size and concentration of TiN on the properties of the composite.

As can be seen from Fig. 4, the addition of the fine-grained TiN accelerates slightly the densification of the material at hot pressing [19]. The reverse is the case for coarse-grained TiN. An improved sintering behaviour of TiN-containing composites can be explained by the formation of a TiO₂-containing low-viscous liquid phase at the initial stage [38] and by the interaction of TiO₂, which is always present on the surface of TiN particles, with Si₃N₄ during hot pressing according to the reactions

$$6TiO_2 + 4Si_3N_4 = 6TiN + 12SiO + 5N_2 \quad (8)$$

$$6TiO_2 + 2Si_3N_4 = 6TiN + 6SiO_2 + N_2 \quad (9)$$
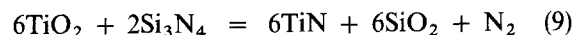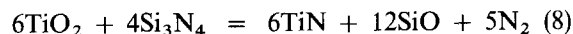
Reaction 9 increases the quantity of the liquid silicate phase during sintering. The formation of titanium-containing SiAlON phases with a low liquidus temperature was also considered for Al₂O₃-containing ceramics [62]. In addition to the interaction with Si₃N₄ and SiO₂, the reaction of TiC with sintering additives should be taken into account

$$2Al_2O_3 + 6TiC + 5N_2 = 4AlN + 6TiN + 6CO \qquad (10)$$

$$2Al_2O_3 + 9TiC + 4.5N_2 = Al_4C_3 + 9TiN + 6CO \qquad (11)$$
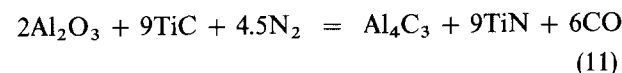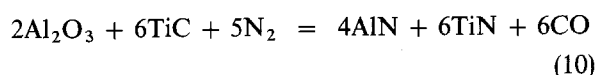
These reactions depend not only on the nitrogen pressure, but also on the partial pressure of CO and on the activity of Al₂O₃ in the liquid phase [38].
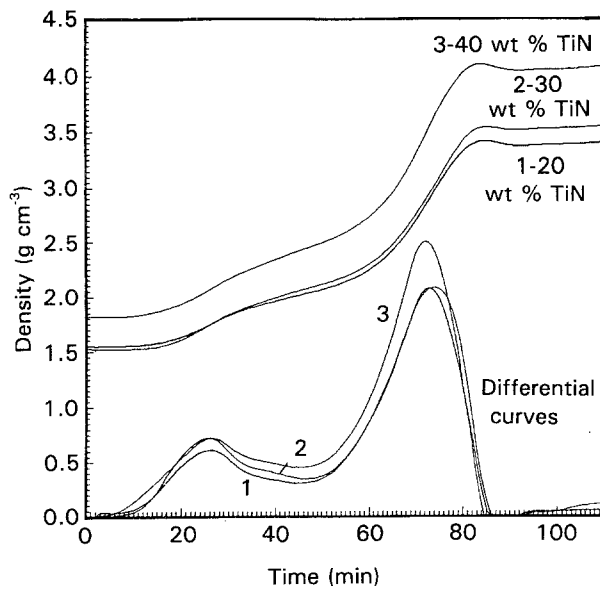
Figure 4 Densification of ceramics with different TiN contents during hot pressing under vacuum [19].

As is known, hot pressing without an inert atmosphere is much cheaper because it does not require expensive vacuum equipment and has a higher productiveness due to a shorter pressing cycle [63]. The main disadvantage of this process is a carbonization of silicon nitride which determines poorer properties of ceramics. To produce the materials by this method, silicon nitride should be protected from reacting with the gas phase (mainly CO formed due to oxidation of graphite) before the formation of closed porosity. From this point of view, the interaction of TiN with the carbon-containing gas atmosphere becomes rather interesting. As is shown by X-ray and Auger spectroscopy of the polished samples hot-pressed under such conditions, TiN grains can bind some amounts of carbon and oxygen [33]. As a result, coarse TiN grains are enveloped by $TiC_xO_yN_z$ and fine grains are apparently not TiN, but the grains of titanium oxycarbonitride. Thus, the TiN particles bonding carbon from the gas phase are capable of decreasing carbonization of the silicon nitride matrix.

In the case of unstable TiC, Reactions 3 and 4 decrease the quantity of the liquid phase in the system and the densification rate [19]. The sinterability of the composites decreases with increasing carbon content in TiC_xN_{1-x} [38].
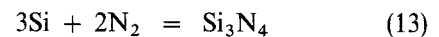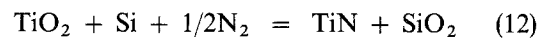
3.2. Sintering

Both pressureless [25, 27] and gas-pressure [27, 35] sintering were successfully used for manufacturing Si_3N_4-based composites. Si_3N_4–TiN composites can be fabricated to densities > 99% by two-step gas pressure sintering [27]. Slip casting was successfully used to produce uniform green structures [27]. The effect of the TiN or TiC content on the shrinkage of the composites is the same as in the case of hot pressing [38]. Fine-grain TiN takes part in the solution–diffusion–precipitation stage of the sintering process and accelerates the densification of silicon nitride.

TiO_2 on the surface of the particles forms an intermediate liquid at the first stage of sintering. At higher temperatures it is reduced to TiN. The increase of the grain size or carbon content in TiC_xN_{1-x} decreases the sinterability of the composite due to instability of the carbonitride under sintering conditions.
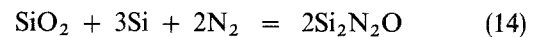
3.3. Reaction sintering

In situ reactions have also been used for preparing composites. A reaction sintering process has been developed to reinforce Si_3N_4 and SiAlONs with refractory nitrides, borides and carbides. This approach can improve hardness and toughness of the material, as well as provide better sintering capabilities. Other advantages include low cost and unique microstructures [64–66].

Nitridation of Si–TiN mixtures allows porous electro-conductive composites to be obtained [29]. This process can be also based [66] on the nitridation of $Si + TiO_2$ mixtures. The reactions

$$TiO_2 + Si + 1/2N_2 = TiN + SiO_2 \quad (12)$$

$$3Si + 2N_2 = Si_3N_4 \quad (13)$$

and

$$SiO_2 + 3Si + 2N_2 = 2Si_2N_2O \quad (14)$$

result in the formation of TiN-reinforced silicon nitride/silicon oxynitride composites [66]. The following reaction [65]

$$Ti_2O_3 + 3AlN + 5Si_3N_4 = 3Si_5AlON_7 + 2TiN \quad (15)$$
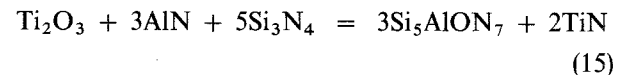
will give a SiAlON composite containing 8 vol % TiN. To produce ceramics with increasing TiN content requires a proportional increase in titanium oxides and hence in the requirement for substitution of oxygen in the β-SiAlON. Alternatively, a less-expensive TiO_2 can be used [65]

$$2TiO_2 + 3AlN + 5Si_3N_4 = 3Si_5AlON_7 + 2TiN + \tfrac{1}{2}O_2 \quad (16)$$
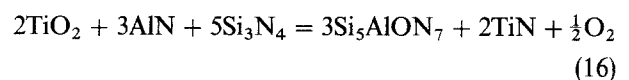
The excess oxygen may be released during the sintering or lead to the formation of TiN_xO_y solid solutions.

The interaction between TiN and BN during sintering in the presence of silicon or SiO_2 will produce TiB_2-containing composites with Si_3N_4 or Si_2N_2O matrices [67]

$$4TiN + 8BN + 9Si = 4TiB_2 + 3Si_3N_4 \quad (17)$$

$$4TiN + 8BN + 9Si + 3SiO_2 = 4TiB_2 + 6Si_2N_2O \quad (18)$$
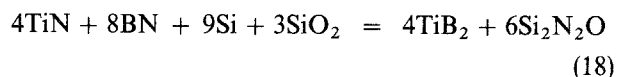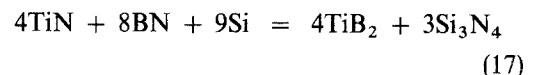
Additions of AlN, Al_2O_3 and/or Y_2O_3 will lead to the formation of β- or α-SiAlON matrices [67]. BN itself can be produced in a SiAlON matrix according to the reaction

$$B_2O_3 + 3AlN + Si_3N_4 = 2BN + Si_3Al_3O_3N_5 \quad (19)$$
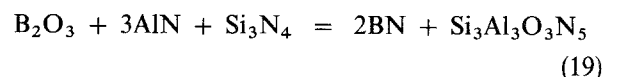
The mixtures of Si_3N_4 and titanium powder can react

producing titanium silicides [68], which have low mechanical properties and are not desirable in the composite. On the other hand, our preliminary experiments demonstrated that nitridation of titanium silicides (Ti_5Si_3 or $TiSi_2$) or mixtures of TiH_2 and silicon [69] can produce Si_3N_4–TiN composites.

An interesting method, which has still not been applied to silicon nitride composites, is the self-propagating high-temperature synthesis [70]. This method allows powders to be obtained as well as porous and even dense (when combined with forging or post-sintering) ceramics [70, 71]. All constituents of the composites, i.e. Si_3N_4 [70] and refractory metals nitrides, borides and carbides [70, 71], can be produced by this method.

Figure 6 Dependence of the lattice parameters of Si_3N_4 and TiN on the TiN content in the HPSN–TiN composites [72]. (□) TiN (222), (△) TiN (331), (·· O ··) Si_3N_4 (322).

4. Microstructure and composition

The studies of the microstructure of TiN-containing ceramics demonstrated that TiN grains in most cases are relatively uniformly distributed in the silicon nitride matrix and form a continuous skeleton at > 30 wt % TiN. Introduction of TiN, ZrN or other compounds that did not interact with Si_3N_4 at sintering temperatures did not affect strongly the composition and structure of the silicon nitride matrix [33, 38]. The typical microstructure of a composite is represented by the silicon nitride matrix with elong-
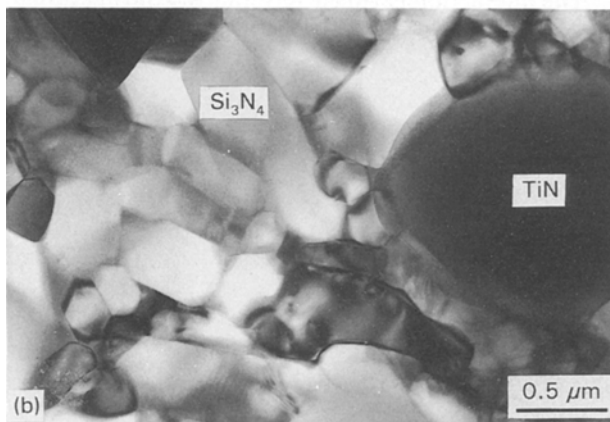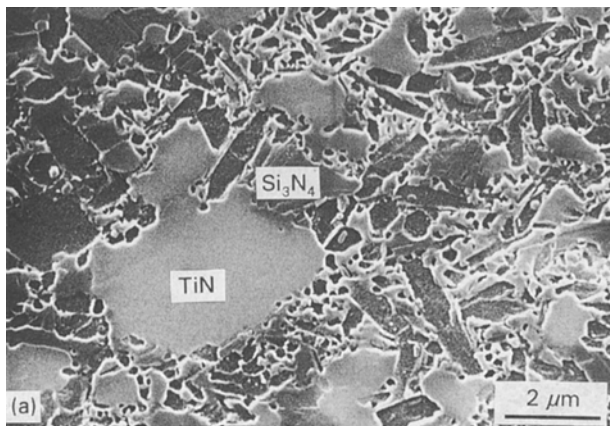
Figure 5 Representative (a) scanning electron micrograph (polished and plasma-etched surface) and (b) transmission electron micrograph showing the microstructure of the HPSN–30TiN composite (30 wt % TiN).
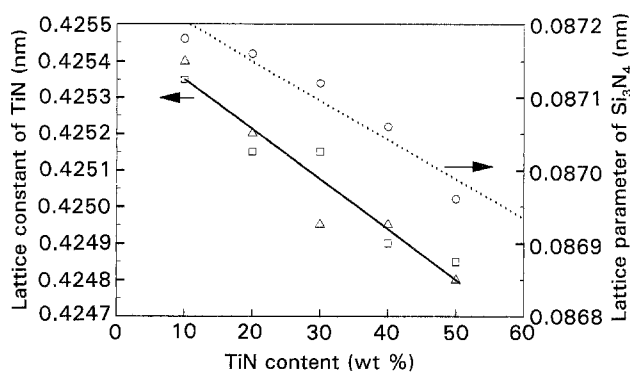
ated β-Si_3N_4 grains and equiaxial TiN grains (Fig. 5a). The average grain size of the silicon nitride matrix was < 1 μm for hot-pressed and sintered ceramics. The transmission electron microscopy (TEM) investigations showed the presence of a glassy or partially crystalline intergranular phase along grain boundaries and in the triple-point junctions (Fig. 5b). No noticeable interaction zone was found between Si_3N_4 and TiN grains. Only a slight decrease of the aspect ratio of β-Si_3N_4 was observed at high contents of the dispersoid. Interaction of TiO_2 on the surface of the particles with sintering aids and with Si_3N_4 according to Equations 8 and 9 can lead to some changes in the composition of the intergranular phase, for example, the formation of Y_2TiO_5 was reported [35]. Changes of the lattice parameter of TiN after sintering were also found [26]. Recent investigations [72] demonstrated that these changes (Fig. 6) occurred as a result of the internal stresses rather than chemical interactions. The decrease of the lattice constants at higher TiN contents can be explained by increasing compression stresses in Si_3N_4 and decreasing tensile stresses in TiN. However, formation of solid solutions during sintering must, of course, also affect the lattice parameters of Si_3N_4 and TiN.

Introduction of carbides or carbonitrides can cause much stronger changes in the composition and microstructure of the matrix due to Reactions 1 and 3. Reaction 1 can lead even to a complete transformation of silicon nitride to silicon carbide [73]. The interaction of carbides with the matrix can be reduced through utilization of coated dispersoids. However, this development route still has not been explored.

5. Effects of added particles on properties

5.1. Specific weight

Silicon nitride has a lower specific weight than nitrides, carbides and borides of transition metals (Table I). Therefore, the specific weight of composites grows with the increasing content of the dispersoid (Fig. 7). This can lead to some limitations in the case of aerospace and other applications of the composites, when the weight of the components is exceptionally important.
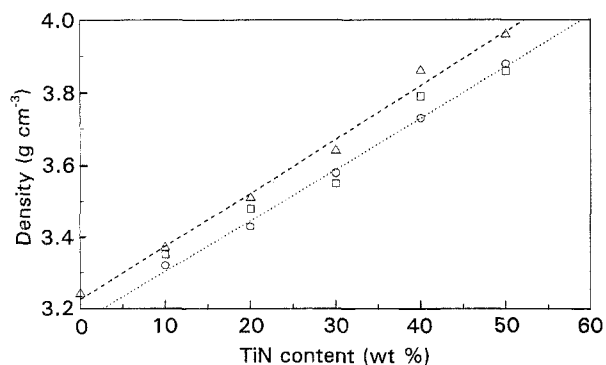
Figure 7 Density versus TiN content for hot-pressed composites with different TiN grain size [33]: (— △ —) 0.83 μm, (·· ○ ··) 2.43 μm, (□) 16.8 μm.

Fig. 7 shows also that the relative density of the composites is almost independent of the TiN content in this concentration range, but decreases slightly with increasing size of TiN particles due to increasing residual porosity. A similar tendency was observed for β-SiAlON–TiN ceramics at TiN concentrations up to 80 vol % [23]. At higher TiN contents, residual porosity after hot pressing increased gradually and the density decreased.

5.2. Electrical conductivity

The relation of conductivity to the dispersoid concentration is characteristic of the materials the structure of which is a heterogeneous mixture of insulating and conductive phases. The electrical conductivity of a mixture of insulating (Si_3N_4) and conductive (dispersoid) particles increases drastically at a certain concentration of the conductive component, the so-called percolation concentration. Among the parameters influencing the percolation concentration, the dispersoid distribution, dispersoid shape and the dispersoid/matrix interactions are the most important ones [74].

The resistivity of Si_3N_4–ZrC composites can vary from $0.001–10^5$ Ωm [75]. Materials with very low resistivity can be also obtained by adding TiN or TiC. The dependencies of the resistivity on the TiN [33] and ZrC [75] contents are shown in Fig. 8. In the region of low dispersoid concentrations, the particles are incorporated in the insulating matrix and the resistivity of the composite is relatively high. At a certain dispersoid content (~ 20 vol % in case of the fine-grained TiN), a network of the conducting phase within the insulating one is formed. As a consequence, the resistivity of the composite shows a drastic decrease to the low value of the conductive network. After the first conductive network is formed, the conductivity shows a slow increase due to improving quality of the conductive network. Metal-like conductivity is observed at lower concentrations in the case of finer TiN grains. This can be explained by the fact that the specific surface area of conductive particles, and accordingly, the surface area of contacts increases with the TiN fineness. The presence of coarse TiN particles leads to breaks in the conductive chains
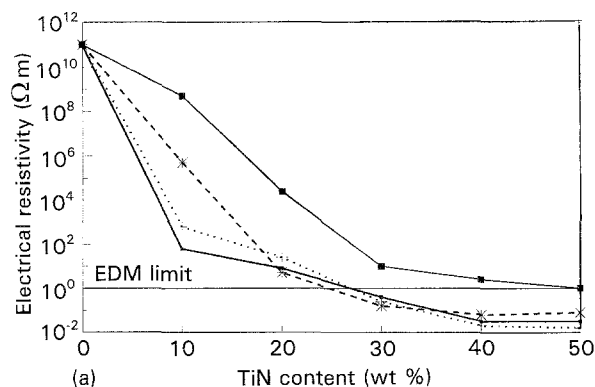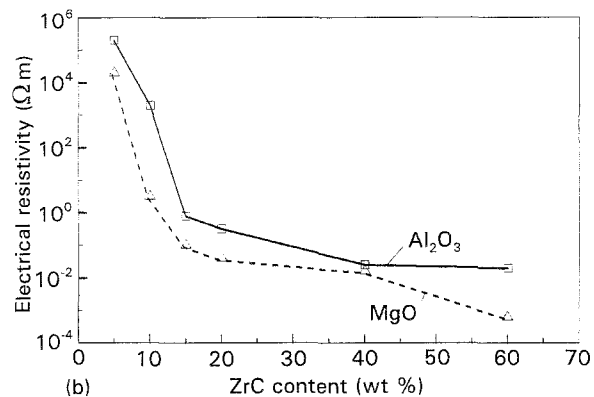
Figure 8 Resistivity as a function of the (a) TiN [33] and (b) ZrC [41] content. (a) (■) b.m. (~ 1 μm), (+) 0.83 μm, (*) 2.43 μm, (■) 36.8 μm.

and the percolation concentration shifts to 40 wt % (Fig. 8). At higher concentrations, the conductivity becomes much less dependent on the TiN grain size.

Conductivity of ceramics depends on the sintering route [35], because it can alter the structure and composition of the composite. Reaction sintering produces electroconductivity with a relatively low volume fraction of TiN (~ 20 vol %) in a SiAlON matrix due to the formation of TiN network structures [65]. Fig. 8b shows that the sintering aids also can affect strongly the conductivity of the composites. MgO-doped ceramics had a higher conductivity than Al_2O_3-doped one with the same content of fine-grained (< 3 μm) ZrC. The oxide additives can change the composition of the grain-boundary phase and exert an influence on the interaction between the matrix and dispersoid.

The temperature coefficient or resistivity was negative for ceramics with low ZrC contents and changed to positive values at 20–40 vol % ZrC [75].

5.2.1. Electrical discharge machining

As can be seen in Fig. 8, ceramics with more than 20 vol % TiN can be EDM-treated. Cutting rates of $1.5–5$ mm min^{-1} were reported for ceramics with 30–50 vol % TiN [25, 35]. The material removal rate was higher than for WC. This demonstrates the high machinability of Si_3N_4–TiN composites. The mechanisms of TiN and Si_3N_4 removal are melting and evaporation respectively [35]. The surface roughness and the damaged layer can be reduced by combining coarse machining with finish machining [25].

5.3. Thermal expansion

The thermal expansion of the composites is always higher than that of Si_3N_4, because of the higher thermal expansion coefficients of the refractory compounds (Table I). It was shown [35] that the experimental values of the thermal expansion coefficient, α, are in good agreement with those calculated with the rule of mixtures according to

$$\alpha = \alpha_m V_m + \alpha_p V_p \qquad (20)$$

where V_m and V_p are the respective volume fractions. The thermal expansion of the Si_3N_4–TiN mixtures grows linearly with increasing TiN content (Fig. 9).

5.4. Mechanical properties
5.4.1. Young's modulus

Most of the refractory compounds are stiffer than Si_3N_4 (Table I). Therefore, regardless of the matrix and sintering route used, the modulus values of the composites, either with coarse or fine TiN powder, increase with increase in the TiN content (Fig. 10). Theoretical models [47] show that the elastic modulus of a composite, E, should be within the range given by

$$E_p E_m/(E_m V_m + E_p V_p) \leqslant E \leqslant E_m V_m + E_p V_p \qquad (21)$$

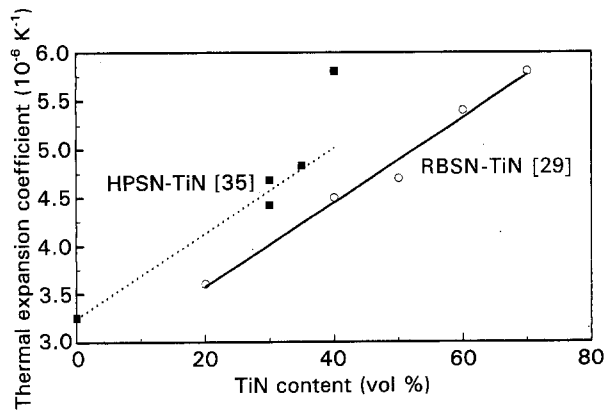where E_m and E_p are the moduli of the matrix and

Figure 9 Thermal expansion coefficient versus TiN content in Si_3N_4–TiN composites.

Figure 10 Young's modulus versus TiN content in hot-pressed and sintered Si_3N_4 and SiAlON-based composites: (—○—) SiAlON–TiN [23], (··□··) HPSN–TiN [34], (–△–) HPSN–TiN [35], (–●–) SSN–TiN [35].

TiN. The lower-bound solution (left-hand) is for the condition where the matrix and particles are equally stressed and the upper-bond solution (right-hand) is for the condition where both phases are equally strained. The experimental values are in agreement with the calculated ones and lie usually within the calculated range between the upper and lower boundaries (Fig. 10). Extrapolation of all dependencies to 100% TiN leads to the same point which is near to the E value for pure TiN (Table I). A slight decrease of E values at > 80 vol % TiN, that was observed for β-SiAlON–TiN composites, can be explained by increasing porosity of the samples or by their spontaneous microcracking, which can occur at high TiN contents [56].

Thus, the elastic modulus, as well as density and thermal expansion, can be estimated with knowledge of the modulus ratio and the volume fraction of the dispersoid. However, pores and cracks, induced during fabrication, can reduce the modulus from the expected values.

5.4.2. Fracture toughness

Additions of even small quantities of nitrides, carbides, borides and silicides can increase the fracture toughness of silicon nitride (Table II). These data are somewhat higher than it was possible to expect taking into account a relatively low density of the composites. Residual porosity can also affect the fracture toughness. Nevertheless, they show that the fracture toughness can be affected by the additives, and that higher values were obtained for dispersoids with a larger grain size.

As was shown in Fig. 2, the concentration dependence of the fracture toughness of composites may have a maximum, which was found experimentally in a number of publications for SiAlON–TiN [24], SiAlON–TiC [14], Si_3N_4–TiC [15], Si_3N_4–TiN [26, 35], and others. Fracture toughness was strongly dependent on the grain size of the composites (Fig. 11). Larger TiC particles yielded a greater toughness than smaller sizes (Fig. 11a), but only a decrease of K_{Ic} was observed in this system. In other investigations [14, 15], an increase in fracture toughness was achieved with coarser (8 μm) dispersoids. The effect of the grain size can be explained by the separation of stress fields due to a greater distance between the particles and therefore a greater amount of crack bowing prior to breakaway. For smaller particles, the stress fields can overlap without significant bowing [47]. It is also necessary to take into account the fact that the crack front can interact only with particles that are larger than the grains of the matrix. It is important also to notice that for coarse particles the maximum fracture toughness will be achieved at lower concentrations of the dispersoid.

A slightly different trend has been reported in the silicon nitride–TiN system (Fig. 11b). The fracture toughness of the composites increased with increasing TiN content and then decreased, in the case of coarse TiN. Ceramics with $D_{50} = 2.43$ μm demonstrated higher K_{Ic} values than other model compositions.

Figure 12 Vickers hardness measured at 98 N as a function of size and concentration of TiN [26].
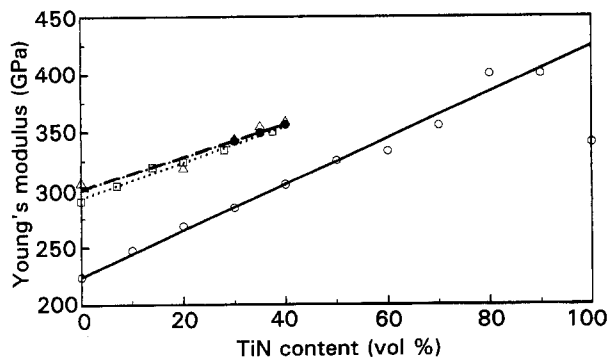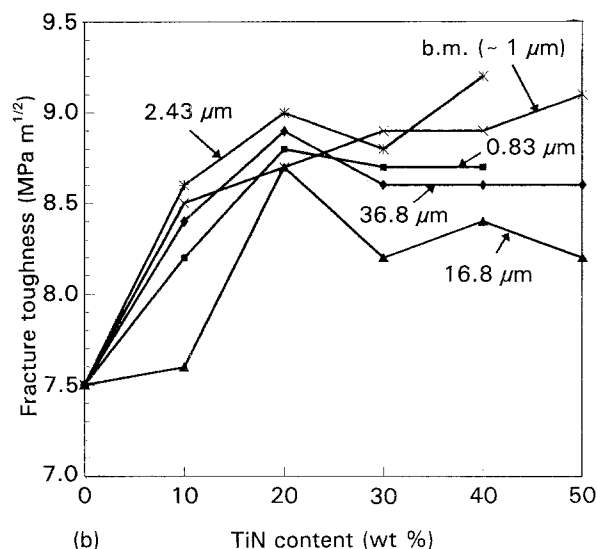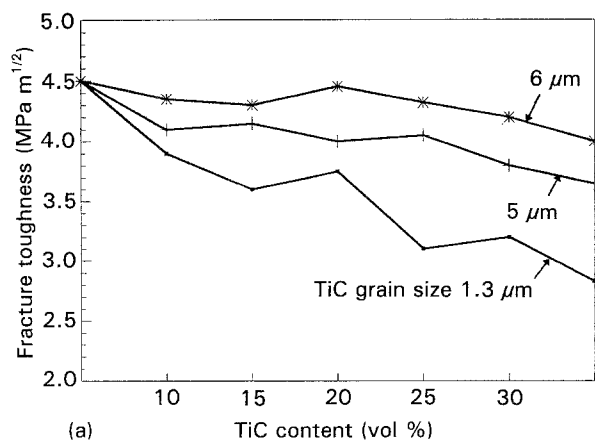
Figure 11 Indentation fracture toughness as a function of size and concentration of the dispersoid in hot-pressed (a) Si_3N_4–TiC [4], and (b) Si_3N_4–TiN [33] composites.

Similarly, the highest K_{Ic} values were measured at a TiN grain size of 3.7 μm in ceramics with 10 vol % TiN ranging from 0.3–13.6 μm [76]. A better pronounced maximum was found in the β-SiAlON–TiN system (Fig. 2). K_{Ic} values from 4 MPa m$^{1/2}$ [77] to 10 MPa m$^{1/2}$ [78] were reported for TiN-containing ceramics. In the concentration range 0–20 vol % TiN, a continuous growth of K_{Ic} with TiN content was found [79].

Another strategy of interest for obtaining a high fracture toughness is based on using mixed whiskers/particles systems. It enables different mechanisms of increasing fracture toughness and work of fracture to be used. A K_{Ic} value of 9.1 MPa m$^{1/2}$ was reached in the Si_3N_4–TiN–SiC$_w$ system [80]. Addition of TiN whiskers which were developed recently [81] could also contribute into improvement of the fracture toughness of the composites.

5.4.3. Hardness

Silicon nitride is a very hard material (Table I). Therefore, hardness generally decreases with an increase in the content of the dispersoid, that is softer than the matrix, e.g. TiN (Fig. 12). Changes in the porosity,
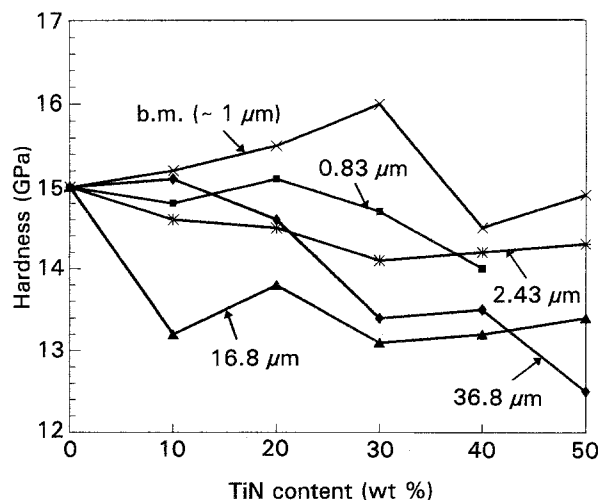
composition and grain size of the matrix, caused by the addition of the dispersed phase, can also strongly affect the hardness of the composite. Thus, additions of fine-grained (< 2 μm) TiC can increase the hardness [4], probably due to a higher hardness of TiC and the formation of hard SiC particles according to Reaction 1. A slight increase of hardness was also found for some Si_3N_4–TiN composites [33]. It should be noted that the hardness of ceramics at high loads, which are necessary in the case of composites with a coarse structure, as opposed to microhardness, is determined not only by elastic–plastic properties of the material, but also by its brittle fracture. Owing to this fact, hardness can correlate with strength. In the case shown in Fig. 12, at a general tendency to lower hardness with a growing TiN content, a certain maximum is observed on the majority of curves at about 20 wt % TiN, i.e. at the concentration corresponding to the maximum strength of these composites.

The hardness also decreased with increasing grain size of TiN. The only exception to the rule was the hardness of the composites with small quantities of coarse TiN (36.8 μm fraction). In this case, most indents were in TiN-free regions, and only a few TiN grains were involved.

5.4.4. Wear resistance

A major focus of particulate composite research has been in the area of tribological applications [63, 82]. β-SiAlON–TiN composite has a friction coefficient of 0.35–0.55 at non-lubricated sliding against steel [83]. No interaction with steel was found at sliding velocities of 1–6 m s^{-1} below 800 °C. Only at higher temperatures did transfer of titanium on to the steel surface occur [84]. The highest wear resistance of the composites was observed at the highest sliding velocities [85].

TiC- or TiN-containing HPSN has a very good abrasive wear resistance (pin-on-ring test on SiC paper [86]). A hot-pressed β-SiAlON–TiN composite possesses a higher wear resistance against corundum

and diamond than AlN and SiC [87]. The wear increases with increase of the diamond grain size and load.

Investigation of the effects of TiN content and grain size demonstrated that ceramics with coarse TiN possess the highest wear resistance at TiN contents less than 40 wt % (Fig. 13). For ceramics with the same TiN distribution, a correlation between the strength, hardness and wear resistance was found [88]. A de-
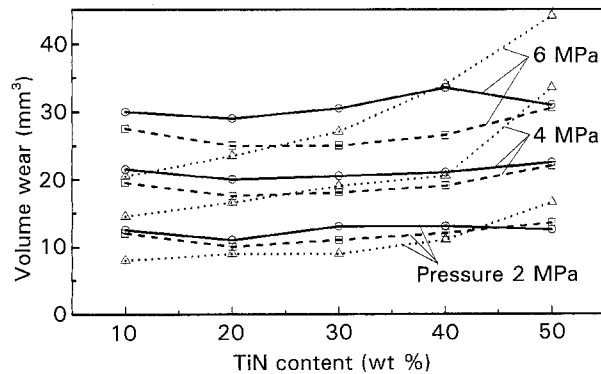
pendence of the abrasive wear on the fracture toughness was not clearly pronounced.

The resistance of hot-pressed cutting tools made from ultra-fine plasmochemical Si_3N_4–TiN powders [61] increases on increasing the TiN content to 25 vol % and decreases again above 70 vol % (Fig. 14). The increase in the wear resistance of TiN-containing ceramics was ascribed [83, 89] to the formation of TiO_2 films on the sliding surface. A lower wear resistance at high concentrations of TiN was caused by a decrease of mechanical properties. In the case of TiN, HfN and ZrN additions [90], no changes of the friction coefficient were found on sliding against steel.

Figure 13 Abrasive wear versus TiN content for composites with fine and coarse TiN tested at different loads [88]. Diamond ring 100/80 μm, pin-on-ring test. (—O—) 0.83 μm, (—□—) 2.43 μm, (·· △ ··) 36.8 μm.

5.4.5. Room-temperature strength

When fine powders are used, the strength of composites is usually the same as that of the matrix [26, 35, 91] or insignificantly altered due to changes of density and flaw size in the material (Table II). A significant improvement in strength (> 50%) was found only for low-strength β-SiAlON matrices made from low-quality β-Si_3N_4 powders [23, 24]. A drastic strength decrease with increasing TiN content was reported only for RBSN–TiN composites [29]. Some of typical concentration dependencies are presented in Fig. 15. Only a slight improvement with the maximum at 20–40 wt % was observed in some cases [35, 92]. The room-temperature bending strength is greatly influenced by the type of TiN powder used. Fractographic studies demonstrated that for the composites with a fine TiN addition, TiN agglomerates acted as fracture origins; while in the case of coarse TiN grains these grains or surface flaws caused by their spalling during grinding became such origins. The non-uniformity of the TiN particle-size distribution which can hardly be avoided in real structures gives rise to the regions of tensile stresses the size of which is larger than a certain limiting value inducing the crack formation. A higher content of the dispersoid results in a larger number and size of agglomerates involving the loss of strength [26, 33, 35, 38]. Therefore, ball-milled (b.m.) ceramics, with a very uniform distribution of TiN in the matrix, possessed much higher
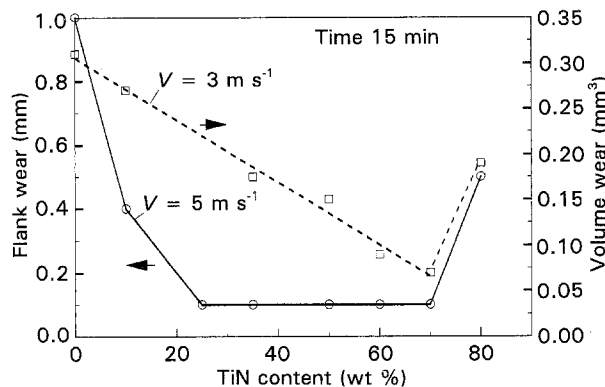

Figure 14 Flank wear of the cutting tool and volume wear of the composite at sliding against steel 45 (0.45% C) as a function of TiN content [84].

TABLE II Effect of dispersoids (5 wt %) on the fracture toughness and strength of pressureless sintered (5% Y_2O_3 + 2% Al_2O_3)-doped silicon nitride [76]

Additive	Grain size of dispersoid (μm)	Density (g cm^{-3})	K_{Ic} (MPa m$^{1/2}$)	Strength (MPa)
HfN	3.85	3.26	7.1	550
Cr$_2$N	3.85	2.96	10.7	520
TiN	1.50	3.03	7.8	590
NbC	1.12	3.06	7.8	590
Cr$_3$C$_2$	4.30	3.07	8.3	420
SiC	0.15	2.88	5.8	590
ZrB$_2$	1.85	2.92	8.8	420
TiB$_2$	1.30	2.80	8.5	480
NbB	3.70	3.06	11.8	570
CrSi$_2$	2.80	2.89	8.0	540
TaSi$_2$	3.40	3.31	11.0	620
ZrSi$_2$	3.65	3.08	11.8	550
None		2.96	7.9	590
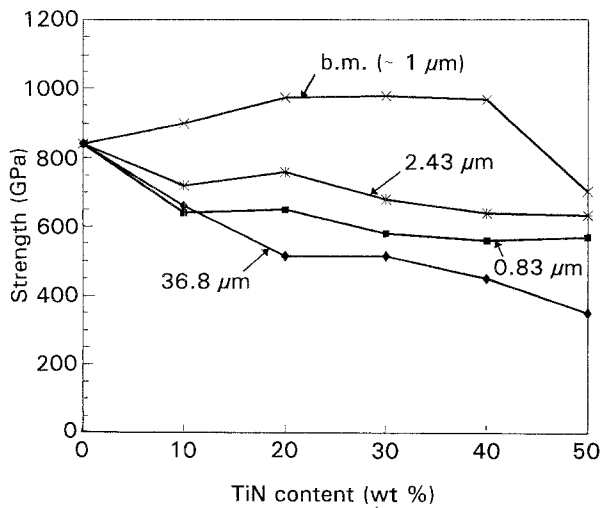
Figure 15 Bending strength as a function of size and concentration of TiN [33, 92].

Figure 16 Temperature dependencies of the three-point bending strength of composites hot-pressed in (a) CO–CO$_2$, and (b) inert atmosphere. Tests in vacuum. (—O—) HPSN, (··□··) HPSN–10TiN, (—△—) HPSN–30TiN, (—··▲—) HPSN–40TiN, (—■—) HPSN–50TiN.

Figure 17 Creep curves of HPSN with different TiN contents at 1250 °C and 100 MPa [92].

strength (Fig. 15) than ceramics with fine-grained TiN (0.83 μm) prepared by short-term mixing and containing agglomerates with the size of 10–50 μm.

It was reported [38] that the addition of TiN can lead to an increase of the Weibull modulus. This can be a result of the change of the flaw population controlling the strength from the surface and intrinsic flaws in the silicon nitride matrix to TiN-related flaws with a narrower size distribution.

5.4.6. High-temperature strength

With increasing temperatures, the level of internal stresses and their effect on strength decrease. The analysis of strength–temperature dependencies (Fig. 16) confirms that their shape corresponds to the classical curves described by Trefilov et al. [93] and is characterized by a maximum at about 800 °C due to a brittle–ductile transition in the intergranular phase and/or TiN. At higher temperatures, the typical strength degradation for silicon nitride ceramics [31, 94, 95] due to softening of the intergranular phase occurs.

Fig. 16 also demonstrates that the materials prepared from the same powder mixtures but using different technological routes can differ strongly in mechanical behaviour. This is connected first of all with changes in the microstructure and composition of the intergranular phase.

5.4.7. Creep

Creep of Si$_3$N$_4$–TiN, –TiC and –TiCN was studied under compression [18, 28, 96] and bending [92, 97, 98]. No information on the tensile creep tests is available. As can be seen in Fig. 17, the increase of TiN content in ceramics leads to higher creep rates, macroscopic deformation and shorter rupture times of the samples. Higher creep rates were measured also for TiC- or TiCN-containing ceramics under compression creep tests [18]. The quasi-stationary creep rates of materials with different TiN contents tested at
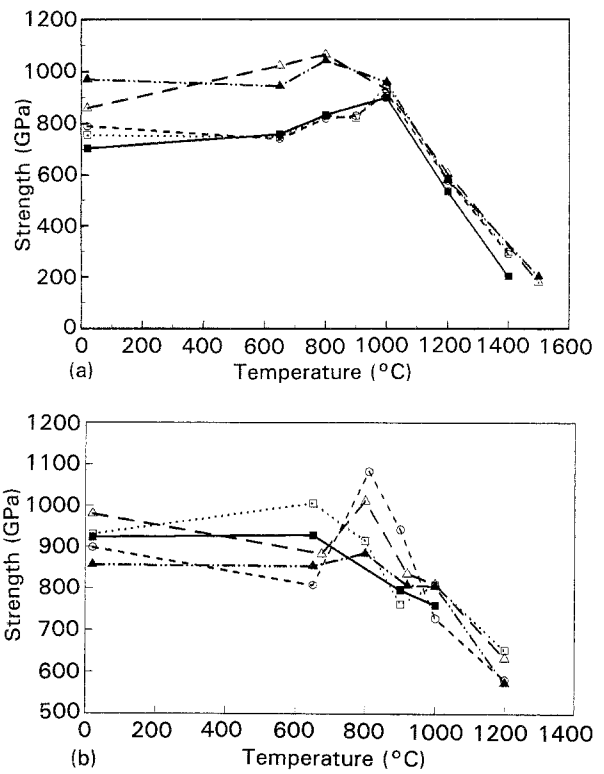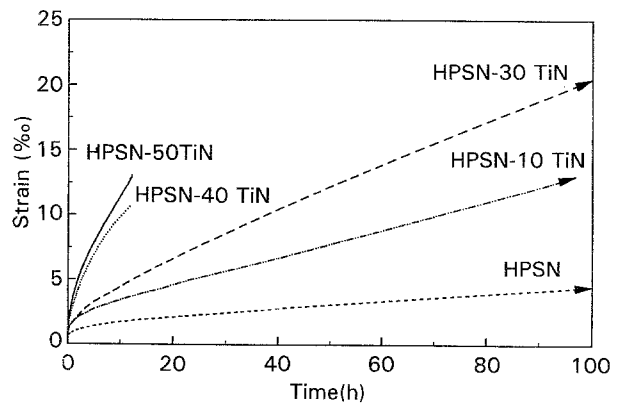
100 MPa are summarized in Fig. 18 as a function of the TiN content. As can be seen from the semilogarithmic plot, a close to exponential dependence of the creep rate on the TiN content is observed. The addition of up to 30 wt % TiN leads only to a slight increase in the creep rate. A stronger change is manifested at higher TiN contents. Probably, the formation of a TiN skeleton at > 30 wt % [26] detrimentally affects the creep behaviour of ceramics. Fine-grained matrix microstructure in the TiN-rich ceramics can also be responsible for the increase of the creep rate. It must be recognized that the effect of TiN additions on the creep rate is dependent upon the temperature. The maximum differences in creep rates were observed at
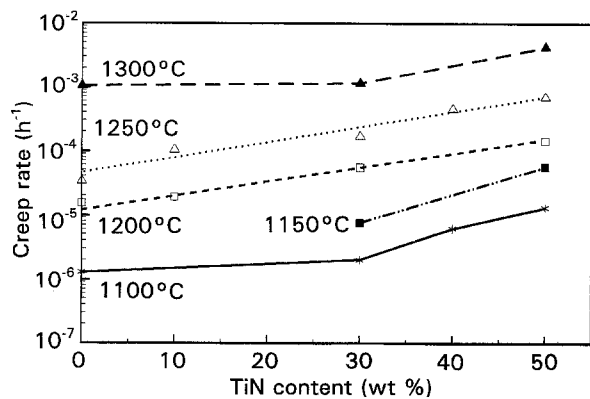
2551

Figure 18 Dependence of the minimum creep rate on the temperature and TiN content in Si_3N_4 ceramics [92].

Figure 19 Mass gain of the TiN-containing HPSN samples oxidized 100 h at 1130 °C versus the content and grain size of TiN [102].

1100 °C. TiN and TiC additions led to changes in the values of stress exponent and apparent activation energy of the materials [96, 97].

On the basis of TEM investigations, it was shown that the steady-state creep rate of the composite can be regarded to be controlled by two creep components, being related to the viscous creep or cavitational accommodation of the matrix, and to the plastic deformation of the TiN [98] or TiC [99] skeleton. However, the deformation of TiN plays a secondary role. The increase of the creep rate with the additive content occurs first of all due to changes in the composition of the intergranular phase. The addition of chemically and plastically active TiC suppresses creep cavitation up to 15% compressive strain [96]. Dislocation activity in TiC grains was much higher than in TiN [99].

The compression creep rate of hot-pressed Si_3N_4-TiB_2 composites at 1600 °C under an inert environment increases with TiB_2 content [100]. A sharp increase of the creep rate was observed at 75 vol % TiB_2 and a superplasticity of this composition was suggested.

5.5. Oxidation

It is known, that the oxidation resistance of carbides and nitrides of refractory metals is lower than that of Si_3N_4 [101]. Therefore, their addition can put limitations on the application of the composites at high temperatures.

The effect of the TiN grain size and content on the oxidation mass gain of HPSN is demonstrated in Fig. 19. The mass gain of composites increases with increasing TiN content. Furthermore, there is a marked increase of oxidative attack with increasing TiN grain size. On the surface of samples with 40 or 50 wt % TiN, the formation of a continuous rutile layer, which has low protective properties, was found (Fig. 20a). The growth of such a scale should be related to the diffusion of titanium to the surface of the composite and its oxidation according to the reaction

$$2TiN + 2O_2 = 2TiO_2 + N_2 \qquad (22)$$

With a decreasing amount of TiN, only those groups of grains that exist near the surface can be
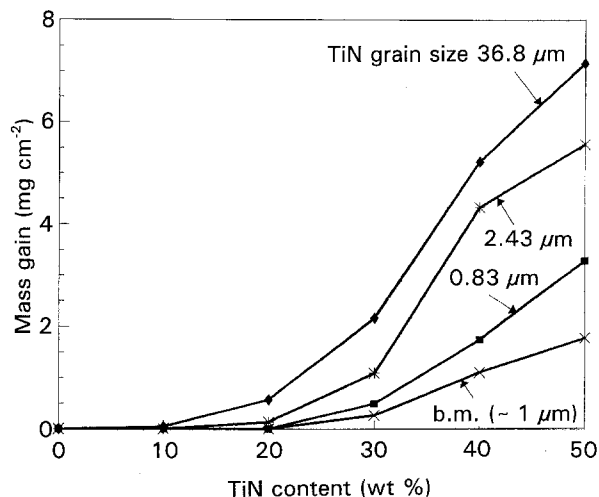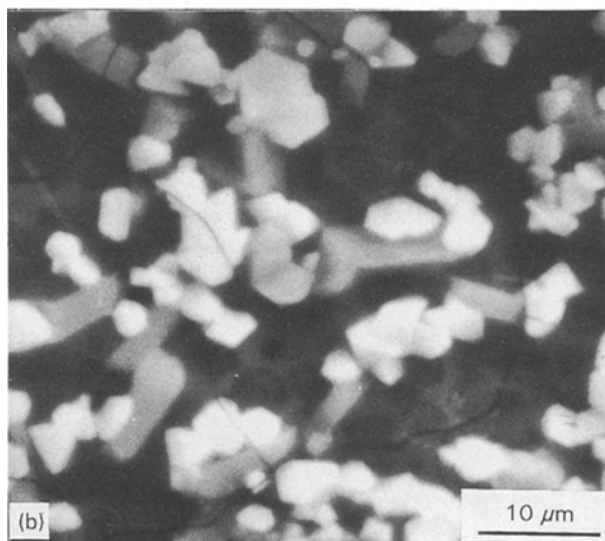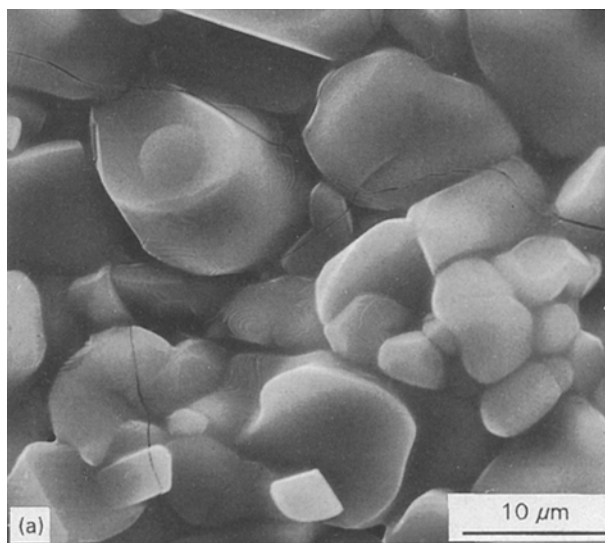

Figure 20 Scanning electron micrographs of the (a) non-protective rutile and (b) protective silicate layers on the surface of (a) HPSN–50TiN and (b) HPSN–30TiN samples after 5 h oxidation at 1300 °C.

oxidized because the TiN grains are present as isolated inclusions in the Si_3N_4 matrix. Rutile islands protruding from the oxide layer were formed in these areas only. Above 1100–1200 °C, the formation of a viscous silicate film (Fig. 20b) on the surface of the composites due to oxidation of silicon nitride according to the reaction

$$Si_3N_4 + 3O_2 = 3SiO_2 + N_2 \qquad (23)$$
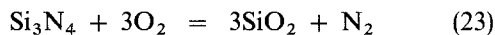
can protect them from further oxidation even at relatively high TiN contents. In this case, the presence of small TiN particles is desirable, because coarse TiN grains prevent the formation of a continuous silicate film on the surface and decrease its protective properties [102, 103]. A correlation between the size of TiN particles in the ceramics and TiO_2 crystals in the oxide layer was observed. These rutile islands, not covered by the silicate film, can work as oxygen pumps, leading to the propagation of the reaction boundary through TiN channels deep inside the material.

It is important to note that the presence of fine isolated inclusions of TiN ($\leqslant 30$ wt %) does not change the mass gain or increases it only slightly, as compared with a TiN-free material (Fig. 19). For materials containing a continuous skeleton of TiN (> 30 wt %) a noticeable increase in the oxidation rate was observed [30, 102–104]. Oxidation of composites can cause a strength decrease at high-temperature tests in air [94] and can be one of the reasons for a lower creep resistance of TiN-rich ceramics [92].

Additions of other compounds, e.g. TiB_2 [42] or TiCN [105], were also deleterious on the oxidation resistance of silicon nitride-based composites. Porous sintered ceramics containing 10%–20% ZrN or 10%–30% TiCN demonstrated a very poor oxidation resistance [36, 37]. Cracking of the ZrN-containing samples occurred after heating in air above 400 °C. This ceramic was easily oxidized also during friction tests [105]. Densification of these ceramics due to additions of sintering aids improved their oxidation resistance. Dense ZrC-containing composites possess high oxidation resistance at least up to 400 °C [41]. Hot-pressed Si_3N_4–ZrN–AlN and Si_3N_4–ZrN ceramics possess a high oxidation resistance up to 1300 °C at ZrN contents less than 10% and 15%, respectively [106]. Hot-pressed β-SiAlON with 42 wt % TiN has relatively high oxidation resistance in air and can survive a short-term heating up to 1700 °C [107, 108]. SiAlON ceramics with 30 wt % $TiSi_2$ demonstrated a higher oxidation resistance at 1100 °C than the same matrix with 30 wt % TiC [109].

6. Applications

The most common application for particulate-reinforced Si_3N_4 is as a tool material [63, 110, 111]. TiN has a low coefficient of friction. Therefore, TiN addition leads to improved wear resistance and extended tool life. The addition of TiC to silicon nitride reduces its solubility in iron [110]. TiN and TiC were traditionally used as coatings [112] and components of alumina-based cutting tools [63, 113]. At present, several types of Si_3N_4-based cutting tools with TiN

and TiCN additions, e.g. SILINIT-R® (IPM, Kiev, Ukraine [63]), TISINIT (ISM, Kiev, Ukraine), WIDIANIT® (Krupp Widia, Germany [86]), are commercially available. TiC- and HfC-containing ceramics with Al_2O_3 and CeO_2 as sintering aids, were also tested as cutting tools [110]. These tools, as well as other silicon nitride tools, are usually used for high-speed cutting and turning of cast iron and nickel-based superalloys. SILINIT-R® tools appeared to be the most promising for high-speed interrupted cutting operations owing to their high fracture toughness and impact resistivity under these conditions [63]. Under the conditions of discontinuous turning of steel (depth of cut 1 mm), the wear resistance of the Si_3N_4–TiN composites is significantly higher than that of monolithic Si_3N_4 [91].

High strength and good strength reproducibility (Weibull modulus > 20 [114, 115]), sufficient fracture toughness (~ 10 MPa m$^{1/2}$) and excellent wear resistance which can be achieved by conventional hot-pressing or sintering make these composites attractive candidates for various tribological and structural components. Experimental parts of Diesel engines, lining and balls for the ball and planetary mills, attritors and disintegrators were made from SiAlON–TiN and Si_3N_4–TiN composites [3, 116]. These composites can replace monolithic silicon nitride in most cases, when a high level of mechanical properties and good machinability are necessary, except for very high-temperature applications (gas turbines, etc.). Ceramic parts made from Si_3N_4–TiN and Si_3N_4–TiB_2 composites can be diffusionally bonded to Incoloy 909® by HIPing at 1200 °C [117]. A higher wear resistance and lower friction coefficient of TiN [86] and TiC-containing composites [118] in comparison with monolithic Si_3N_4 allows their use for sealings, bearings and other wear-resistant parts.

Ceramics with high conductivity can be used for some specific electrotechnical applications. Heaters, collecting electrodes and collector rings from reaction-sintered Si_3N_4–TiN were developed in the Hitachi Research Laboratory [29, 119]. A combination of the electroconductive Si_3N_4–TiN and resistive Si_3N_4–Al_2O_3 compositions was successfully used for manufacturing of commutators [29]. All these parts can be fabricated in near-net-shape.

7. Conclusion

The analysis of the published data shows promise of further investigations of silicon nitride-based particulate composites as structural, tool or electronic materials. These data point to the presence of strong grain boundaries, limited interactions and the mechanism of dispersion toughening in the studied systems. Additions of carbides, nitrides, borides and silicides of transition metals increase the electrical conductivity, Young's modulus, specific weight and thermal expansion coefficient of the composite and decrease its oxidation resistance, high-temperature strength and creep resistance. Sinterability, strength, fracture toughness, hardness and wear resistance can be increased or decreased depending on the type, content

and grain size of the dispersoid. However, only Si_3N_4–TiN and Si_3N_4–TiC systems are studied more or less systematically. For other systems, only limited data were obtained. While some of the properties of composites, e.g. Young's modulus, thermal expansion and density, can be estimated with fair accuracy knowing the properties of the matrix and dispersoid, for other properties experimental verification is necessary.

Particulate composites appear very competitive to other classes of composites in terms of raw material cost and simplified processing. The alteration of the Si_3N_4 microstructure by the dispersed additions may offer a potential for improvement of the composite's properties at room temperature, but the effect at elevated temperature may be adverse. The improvement of technology providing homogeneous mixtures and uniformly distributed particles will ensure a higher level of mechanical properties. The properties can be optimized by varying particulate size and volume loading. However, the improvement in fracture toughness associated with the particulate reinforcement is less than that associated with whiskers or fibres. At the same time, particulate composites are easier processed by any method, that can be used for silicon nitride ceramics.

There is a need for further investigations of the properties of particulate composites. Effects of the additions of carbides and nitrides of transition metals on thermal shock resistance, fracture toughness at elevated temperatures and thermophysical properties have not been investigated. A nanocomposite approach and/or combination of the particles with whiskers or fibres may be feasible for further improvement in mechanical properties.

References
1. F. THÜMMLER, *J. Europ. Ceram. Soc.* **6** (1990) 139.
2. F. PORZ, *Technol. Manage.* [4] (1990) 13.
3. Yu. G. GOGOTSI, "Structural Ceramics: Manufacturing, Properties, Application" (Znanie, Kiev, 1990).
4. S. T. BULJAN and V. K. SARIN, *Composites* **18** (1987) 99.
5. S. T. BULJAN and J. G. BALDONI, *Mater. Sci. Forum* **47** (1989) 249.

6. S. T. BULJAN and G. ZILBERSTEIN, in "Advanced Structural Ceramics", edited by P. F. Becher, M. V. Swain and S. Somiya (MRS, Pittsburgh, PA, 1987) pp. 273–81.
7. R. POMPE, in "Proceedings of the 11th Risø International Symposium on Metallurgy and Materials Science", edited by J. J. Bentzen (Risø National Laboratory, Roskilde, 1990), p. 97.
8. F. F. LANGE, *J. Am. Ceram. Soc.* **56** (1973) 445.
9. C. GRESHKOVICH and J. A. PALM, *ibid.* **63** (1980) 597.
10. J. C. SCHUSTER and H. NOWOTNY, in "Proceedings of the 11th Plansee Seminar", Vol. 1 (1985) pp. 899–911.
11. "Ceramic Material", Sov. Pat. 537 986 (Institute for Problems of Materials Science, Kiev, 1975).
12. "Ceramic Tool Material", Sov. Pat. 689 113 (Institute for Problems of Materials Science, Kiev, 1978).
13. G. G. GNESIN, I. I. OSIPOVA, V. P. YAROSHENKO and G. D. RONTAL, *Poroshk. Metall.* [2] (1978) 48.
14. O. N. GRIGOR'EV, S. I. CHUGUNOVA, A. M. SHATOKHIN and V. P. YAROSHENKO, *ibid.* [7] (1981) 73.
15. T. MAH, M. G. MENDIRATTA and H. A. LIPSITT, *Am. Ceram. Soc. Bull.* **60** (1981) 1229.
16. G. ZILBERSTEIN and S. T. BULJAN, in "Advances in Materials Characterization II, Materials Science Research", Vol. 19, edited by R. S. Snyder, R. A. Condrate and P. F. Johnson (Plenum Press, New York, 1985) p. 389.
17. S. T. BULJAN and G. ZILBERSTEIN, in "Tailoring of Multiphase and Composite Ceramics", Materials Science Research, Vol. 20, edited by R. E. Tressler *et al.* (Plenum Press, New York, 1986) p. 305.
18. F. PENI, J. CRAMPON, R. DUCLOS and B. CALES, *J. Europ. Ceram. Soc.* **8** (1991) 311.
19. M. HERRMANN, Ch. SCHUBERT, J. PABST, H.-J. RICHTER, P. OBENAUS and V. P. JAROSCHENKO, in "Verstärkung keramischer Werkstoffe", Hamburg, 8–9 October 1991 (DGM-Informationsgesellschaft Verlag, Oberursel, 1991) pp. 235–48.
20. "Powder Mixture for the Tool Material", Soviet Pat 919 289 (Institute for Problems of Materials Science, Kiev, 1981).
21. "Ceramic Tool Material", Sov. Pat. 1152 196 (Institute for Problems of Materials Science, Kiev, 1983).
22. E. KAMIJO, M. HONDA, M. HIGUCHI, H. TAKEUCHI and T. TANIMURA, *Sumitomo Electr. Tech. Rev.* **24** (1985) 183.
23. O. V. BAKUN, O. N. GRIGOR'EV, G. G. GNESIN, I. I. OSIPOVA, S. A. FIRSTOV and V. P. YAROSHENKO, *Poroshk. Metall.* [1] (1987) 45.
24. O. V. BAKUN, A. VERSCHTEDT, O. N. GRIGOR'EV, G. KREHER, V. I. TREFILOV, D. SHNEIDER and V. P. YAROSHENKO, *ibid.* [6] (1987) 71.
25. C. MARTIN, B. CALES, P. VIVIER and P. MATHIEU, *Mater. Sci. Eng.* **A109** (1989) 351.
26. V. P. YAROSHENKO, I. I. OSIPOVA, Yu. G. GOGOTSI and D. A. POGORELOVA, in "Tagungsband IX Internationale Pulvermetallurgische Tagung", B. 3 (Dresden, 1989) p. 295.
27. H. MOSTAGHACHI, in "Euro-Ceramics", edited by G. de With, R. A. Terpstra and R. Metselaar (Elsevier, London, 1989) p. 1.410.
28. J. CRAMPON, R. DUCLOS and P. VIVIER, *ibid.* p. 3.298.
29. Y. YASUTOMI and M. SOBUE, *Ceram. Eng. Sci. Proc.* **11** (1990) 857.
30. A. BELLOSI, A. TAMPIERI and Yu-Zh. LIU, *Mater. Sci. Eng.* **A127** (1990) 115.
31. Yu. G. GOGOTSI, O. N. GRIGORJEW and W. P. JAROSCHENKO, *Silikattechnik* **41** (1990) 156.
32. C. J. SHIH, J.-M. YANG and A. EZIS, *Scripta Metall.* **24** (1990) 24119.
33. V. YAROSHENKO, Yu. GOGOTSI and I. OSIPOVA, in "Ceramics Today – Tomorrow's Ceramics", edited by P. Vincenzini (Elsevier, Amsterdam, 1991) p. 2821.
34. Yu. G. GOGOTSI, O. N. GRIGOR'EV and V. P. YAROSHENKO, in "Abstracts of the 2nd European Conference on Advanced Materials and Processes" (Institute of Metals, London, 1991) p. 207.

35. A. BELLOSI, S. GUICCIARDI and A. TAMPIERI, *J. Europ. Ceram. Soc.* **9** (1992) 82.

36. Yu. G. GOGOTSI, V. K. KAZAKOV, V. A. LAVRENKO, T. G. PROTSENKO and V. V. SHVAIKO, *Sov. J. Superhard Mater.* **10** (1988) 33.

37. Yu. G. GOGOTSI and V. A. LAVRENKO, *High Temp. Technol.* **6** (1988) 79.

38. M. HERRMANN, B. BALZER, Ch. SCHUBERT and W. HERMEL, *J. Europ. Ceram. Soc.* **12** (1993) 287.

39. S. SŌMIYA, M. YOSHIMURA and N. SHINOHARA, *Report Res. Lab. Engineering Materials, T.I.T.* **6** (1981) 107.

40. H. J. SEIFERT, M. J. HOFFMANN, H. L. LUKAS and G. PETZOW, in "Proceedings of the 2nd Conference of the European Ceramic Society", Augsburg, 1991 (D. G. Köln, 1993) pp. 131–35.

41. G. G. GNESIN, E. I. GERVITS, L. A. SHIPILOVA, V. Ya. PETROVSKII and A. A. KAS'YANENKO, *Sov. Powder Metall. Metal Ceram.* **29** (1990) 483.

42. A. TAMPIERI, A. BELLOSI and V. BIASINI, in "Material Science Monographs", Vol. 68, "Advanced Structural, Inorganic Composites", edited by P. Vincenzini (Elsevier, New York, 1991) pp. 409–20.

43. Yu. G. GOGOTSI, I. I. OSIPOVA, S. I. CHUGUNOVA and V. Zh. SHEMET, *Sov. Powder Met. Metal Ceram.* **26** (1986) 163.

44. M. YOSHIMURA, N. MORITA, N. NISHIOKA, N. ISHIZAWA and S. SŌMIYA, *J. Ceram. Soc. Jpn* **97** (1989) 910.

45. T. KATO, M. YOSHIMURA and S. SŌMIYA, *Report Res. Lab. Eng. Mater. T.I.T.* **11** (1986) 45.

46. *Idem, Yogyo-Kyokai-shi* **89** (1981) 221.

47. F. F. LANGE, *Philos. Mag.* **22** (1970) 983.

48. A. G. EVANS, *ibid.* **26** (1972) 1327.

49. D. J. GREEN, P. S. NICHOLSON and J. D. EMBURY, *J. Mater. Sci.* **14** (1979) 1657.

50. K. T. FABER and A. G. EVANS, *Acta Metall.* **31** (1983) 565.

51. *Idem, ibid.* **31** (1983) 577.

52. *Idem, J. Am. Ceram. Soc.* **67** (1984) 255.

53. D. J. GREEN, *ibid.* **66** (1983) C-4.

54. A.G. EVANS, *Mater. Sci. Eng.* **A105/106** (1988) 65.

55. M. V. SWAIN, *Mater. Forum* **13** (1989) 237.

56. B. A. GALANOV and O. N. GRIGOR'EV, "Failure of the Elastic-Deformed Solid Heterophase Materials with the Periodic Microstructure" (IPM, Kiev, 1990).

57. G. V. SAMSONOV and I. M. VINITSKII, "Handbook of Refractory Compounds" (IFI/Plenum, New York, 1980).

58. R. C. WEST, ed. "Handbook of Chemistry and Physics", 69th Edn (CRC Press, Cleveland, OH, 1988).

59. W. S. WILLIAMS and R. D. SHAAL, *J. Appl. Phys.* **33** (1962) 955.

60. D. J. MAGLEY, R. A. WINHOLTZ and K. T. FABER, *J. Am. Ceram. Soc.* **73** (1990) 1641.

61. I. I. OSIPOVA, A. M. KOVAL'CHENKO and L. L. SARTINSKAYA, *Poroshk. Metall.* [4] (1992) 46.

62. V. PETROVSKI, in "Key Engineering Materials", Vols 89–91, edited by M. J. Hoffmann, P. F. Becher and G. Petzow (Trans Tech, 1994) pp. 455–60.

63. G. G. GNESIN (ed.), "Ceramic Tool Materials" (Kiev, Tekhnika, 1990).

64. L. M. SHEPPARD, *Am. Ceram. Soc. Bull.* **72** [4] (1993) 48.

65. F. HONG, R. J. LUMBY and M. H. LEWIS, *J. Europ. Ceram. Soc.* **11** (1993) 48.

66. W. LIN, J.-M. YANG, S.-J. TING, A. EZIS and C. J. SHIH, *J. Am. Ceram. Soc.* **75** (1992) 2945.

67. F. HOHG and M. H. LEWIS, in "Processing of Engineering Ceramics" (American Ceramic Society, Westerville, 1993) in press.

68. I. GOTMAN and E. Y. GUTMANAS, *J. Mater. Sci. Lett.* **9** (1990) 813.

69. Yu. G. GOGOTSI, V. P. YAROSHENKO and R. A. MOROZOVA, "Composition of the Silicon Nitride-Based Ceramic and Method of Making the Material", Sov. Pat. 1669900 (1989).

70. J. SUBRAHMANYAM and M. VIJAYKUMAR, *J. Mater. Sci.* **27** (1992) 6249.

71. A. G. MERZHANOV, in "Combustion and Plasma Synthesis of High-temperature Materials", edited by Z. A. Munir and J. B. Holt (VCH, New York, 1990) p. 1.

72. O. N. GRIGOR'EV, G. S. KRIVOSHEY, N. I. PEREPELITSA and L. L. KHOROSHUN, *Zavodsk. Laborat.* [10] (1992) 37.

73. A. KAMIYA and K. NAKANO, *J. Mater. Sci. Lett.* **12** (1993) 430.

74. F. LUX, *J. Mater. Sci.* **28** (1993) 285.

75. G. G. GNESIN, E. I. GERVITS, L. A. SHIPILOVA, V. Ya. PETROVSKII and A. A. KAS'YANENKO, *Poroshk. Metall.* [4] (1990) 80.

76. T. NAGAOKA, M. YASUOKA, K. HIRAO and S. KANZAKI, *J. Ceram. Soc. Jpn* **100** (1992) 617.

77. M. NAKAMURA, A. YOSHIDA, Y. NAKAJIMA, in "Proceedings of the 7th Symposium on Fundamental Technology for Next Generation", Tokyo, 20–21 November 1988, pp. 11–20.

78. K. KISHI and S. UMEBAYASHI, *Nihon Seramikkusu* **96** (1988) 725.

79. T. EKSTRÖM, in "Key Engineering Material", Vols 89–91, edited by M. J. Hoffmann, P. F. Becher and G. Petzow (Trans Tech, 1994) pp. 327–332.

80. Y. SATO and M. UEKI, *J. Ceram. Soc. Jpn* **101** (1993) 365.

81. J. ZHU, X.-G. NING, H.-G. XU *et al., J. Mater. Sci.* **26** (1991) 3202.

82. G. ZIEGLER, Ceramic Forum International, *Bericht. Deutsch. Keram. Ges.* **68** (1991) 399.

83. Yu. G. GOGOTSI, A. M. KOVAL'CHENKO, I. A. KOSSKO and V. P. YAROSHENKO, *Sov. J. Frict. Wear* **11** [4] (1990) 74.

84. A. M. KOVAL'CHENKO, Cand. Science Thesis, Kiev, IPM (1992).

85. A. M. KOVAL'CHENKO, I. I. OSIPOVA, Yu. G. GOGOTSI, V. P. YAROSHENKO and G. N. SAVRANSKAYA, *Trenie i Iznos* **13** (1992) 654.

86. D. HOLZ, R. JANSSEN, K. FRIEDRICH and N. CLAUSSEN, *J. Europ. Ceram Soc.* **5** (1989) 229.

87. A. M. KOVAL'CHENKO, Yu. G. GOGOTSI and V. P. YAROSHENKO, in "Mechanics and Physics of Fracture of Brittle Materials", edited by S. A. Firstov (IPM, Kiev, 1992) pp. 99–105.

88. Yu. G. GOGOTSI, A. M. KOVAL'CHENKO, I. I. OSIPOVA, V. P. YAROSHENKO and V. A. GONCHARUK, *Sverkhtverdye Mater.* [3] (1992) 20.

89. I. DÖRFEL, W. GESATZKE, W. ÖSTERLE and A. SKOPP, in "Key Engineering Materials", Vols 89–91, edited by M. J. Hoffmann, P. F. Becher and G. Petzow (Trans Tech, Aedermannsdorf, 1994) pp. 763–7.

90. D.-S. PARK, H.-D. KIM, S.-Y. LEE and S. KIM, *ibid.*, pp. 439–44.

91. M. HERRMANN, A. BEGER, Chr. SCHUBERT, W. HERMEL, E. MEISSNER and G. ZIEGLER, in "Materials by Powder Technology. PTM'93", edited by F. Aldinger (DGM-Informationsgesellschaft-Verlag, Oberursel, 1993) pp. 779–84.

92. Yu. G. GOGOTSI and G. GRATHWOHL, *J. Mater. Sci.* **28** (1993) 4279.

93. V. I. TREFILOV, Yu. V. MILMAN and I. V. GRIDNEVA, *Crystal Res. Technol.* **19** (1984) 413.

94. V. I. TREFILOV, Yu. G. GOGOTSI, O. N. GRIGOR'EV, V. P. YAROSHENKO, V. A. GONCHARUK and D. Yu. OSTROVOI, *Sov. Powder Metall. Metal Ceram.* **30** (1991) 158.

95. G. ZIEGLER, J. HEINRICH and G. WÖTTING, *J. Mater. Sci.* **22** (1987) 3041.

96. J. CRAMPON and R. DUCLOS, *Acta Metall. Mater.* **38** (1990) 805.

97. Yu. G. GOGOTSI, G. GRATHWOHL and F. PORZ, in "Mechanische Eigenschaften keramischer Konstruktionswerkstoffe", edited by G. Grathwohl (DGM Informationsgesellschaft, Oberursel, 1993) pp. 185–190.

98. Yu. G. GOGOTSI, G. GRATHWOHL and G. E. KHOMENKO, in "Key Engineering Materials", Vols 89–91, edited by M. J. Hoffmann, P. F. Becher and G. Petzow (Trans Tech, Aedermannsdorf, 1994) pp. 659–64.

99. F. PENI, J. CRAMPON and R. DUCLOS, *Ceram. Int.* **18** (1992) 413.

100. R. A. ANDRIEVSKI, V. T. IVANNIKOV and V. S. URBANOVICH, in "Key Engineering Materials", Vols 89–91, edited by M. J. Hoffmann, P. F. Becher and G. Petzow (Trans Tech, Aedermannsdorf, 1994) pp. 445–8.

101. R. F. VOITOVICH, "Oxidation of carbides and nitrides" (Naukova Dumka, Kiev, 1981).

102. Yu. G. GOGOTSI and F. PORZ, *Corrosion Sci.* **33** (1992) 627.

103. Yu. G. GOGOTSI, G. GRATHWOHL, F. PORZ, V. V. KOVYLYAEV and A. D. VASIL'EV, in "Proceedings of the 2nd International Conference on Microscopy of Oxidation" (Institute of Materials, London, 1993) pp. 535–44.

104. Yu. G. GOGOTSI, G. DRANSFIELD and F. PORZ, *Oxid. Metals* **39** (1993) 69.

105. Yu. G. GOGOTSI, V. A. LAVRENKO, "Corrosion of High-Performance Ceramics" (Springer, Berlin, 1992).

106. Ch.-Ch. GE, W.-S. LIU, Y.-L. XIA and L.-M. CHEN, in "Key Engineering Materials", Vols 89–91, edited by M. J. Hoffmann, P. F. Becher and G. Petzow (Trans Tech, Aedermannsdorf, 1994) pp. 307–12.

107. Yu. G. GOGOTSI, O. N. GRIGOR'EV and V. L. TIKUSH, *Sov. Powd. Met. Metal Ceram.* **27** (1988) 386.

108. Yu. G. GOGOTSI, V. A. LAVRENKO, T. G. PROTSENKO, A. I. STEGNIJ and V. L. TIKUSH, *Sverkhtverdye Mater.* [3] (1989) 22.

109. S. A. GIESKIS and M. TERPSTRA (eds.), "Reinforced Ceramic Composites" (Elsevier, London, 1991).

110. S. T. BULJAN and S. F. WAYNE, *Adv. Ceram. Mater.* **2** (1987) 813.

111. A. BELLOSI, *Adv. Ceram. Glass* **1** (1990) 18.

112. S. CHATTERJEE, S. CHANDRASHEKHAR and T. S. SUDARASHAN, *J. Mater. Sci.* **27** (1992) 3409.

113. T. KOYAMA and A. NISHIYAMA, in "Ceramics Today – Tomorrow's Ceramics", edited by P. Vincenzini (Elsevier, Amsterdam, 1991) p. 2841.

114. H. MOSTAGHACI and R. LANGLOIS, in "Ceramic Transactions. Ceramic Powder Science IV", Vol. 22, edited by S. Hirano, G. L. Messing and H. Hausner (American Ceramic Society, Westerville, 1991) p. 655.

115. *Idem*, in "Material Science Monographs", Vol. 68, "Advanced Structural, Inorganic Composites", edited by P. Vincenzini (Elsevier, New York, 1991) pp. 573–81.

116. Yu. G. GOGOTSI, *Adv. Ceram. Glass* [3] (1991) 6.

117. R. LARKER, L.-Y. WEI, M. OLSSON *et al.*, in "Proceedings of the 4th International Symposium on Ceramic Materials and Components for Engines", 1992, Vol. 4, pp. 340–7.

118. P. A. PAGE, C. R. BLANCHARD-ARDID and W. WEI, *J. Mater. Sci.* **23** (1988) 946.

119. Y. YASUTOMI, K. NAKAMURA, M. SOBUE and Y. KUBO, *J. Ceram. Soc. Jpn, Int. Ed.* **97** (1989) 145.